



Artifacts Introduced in the Point Evaluation of Functions Expanded into a Degree 360 Spherical Harmonic Series

R. Rapp

*Department of Civil and Environmental Engineering and Geodetic Science
The Ohio State University, Columbus, Ohio*

National Aeronautics and
Space Administration

Goddard Space Flight Center
Greenbelt, Maryland 20771

Acknowledgments

The preparation of this report was supported by NASA (Contract NAS5-32352) through Raytheon ITSS. Dick Peltier kindly provided the data that was initially analyzed by C. Zhang. H-Z Tseng pointed out the problem with the spurious signal in a degree 360 expansion provided by the author. Nikos Pavlis kindly provided suggestions that led to clarifications of the original text and provided the figure in the Appendix. C. Cox created this document from a variety of text and figure files.

Available from:

NASA Center for AeroSpace Information
Parkway Center/7121 Standard Drive
Hanover, Maryland 21076-1320
Price Code: A17

National Technical Information Service
5285 Port Royal Road
Springfield, VA 22161
Price Code: A10

TABLE OF CONTENTS

Abstract.....	1
Introduction.....	1
Numerical Results for the Expansion of a Function Given in $1^\circ \times 1^\circ$ Cells.....	3
Examination of the EGM96 Geopotential Model for Solution Artifacts in Point Values.....	9
Conclusions.....	15
References.....	17
Appendix.....	19

LIST OF TABLES

Table 1. $1^\circ \times 1^\circ$ Mean Values of rad_dot.M2 Computed From Five Spherical Harmonic Expansions. Units are mm/yr.....	8
Table 2. Square Root of Spectral Power and Differences for Various Expansions of rad_dot.M2. Units are mm/yr.....	8
Table 3. 30' Free-Air Anomalies in US Test Area	13

LIST OF FIGURES

Figure 1. Values of rad_dot.M2 based on a 0.5° grid of point values from the full degree 360 expansion of the 30' mean values. Contour interval is 1 mm/yr.....	4
Figure 2. Values of rad_dot.M2 based on a 0.5° grid of point values from the truncated to 180 360 expansion of the 30' mean values. Contour interval is 1 mm/yr.....	5
Figure 3. Values of rad_dot.M2 based on a 0.5° grid of point values computed from the degree 180 expansion of the $1^\circ \times 1^\circ$ mean values. Contour interval is 1 mm/yr.....	5
Figure 4. Values of rad_dot.M2 based on a 0.5° grid of point values from degree 181 to 360 expansion of the 30' mean values. Contour interval is 1 mm/yr.....	6
Figure 5. Values of rad_dot.M2 based on a 0.5° grid of point values from the degree 181 to 360 expansion of the 30' spline interpolated mean values. Contour interval is 0.1 mm/yr.....	6
Figure 6. Point values of rad_dot.M2 from degree 360 (30' direct) (top value), degree 180 (1° data) (middle value) and degree 360 (30' spline) (lower value) expansion on a 30' grid. Units are mm/yr.....	7
Figure 7. Values of gravity anomaly contribution from degree 181 to 360 from EGM96. Contour interval is 4 mGal.....	10
Figure 8. Values of geoid undulation contribution from degree 181 to 360 from EGM96. Contour interval is 10 cm.....	10
Figure 9. Value of the gravity anomaly from the EGM96 geopotential model in a small Antarctic region. Contour interval is 2 mGal.....	11
Figure 10. Value of the gravity anomaly contribution from degree 181 to 360 from EGM96 in a small Antarctic region. Contour interval is 2 mGal.....	12
Figure 11. Value of the geoid undulation contribution from degree 181 to 360 from EGM96 in a small Antarctic region. Contour interval is 5 cm.....	12
Figure 12. Value of the gravity anomaly from EGM96 in a US test region. Contour interval is 10 mGal.....	14
Figure 13. Value of the gravity anomaly contribution from degree 181 to test region. Contour interval is 5 mGal.....	14

ABSTRACT

An expansion of a function initially given in 1° cells was carried out to degree 360 by using 30' cells whose value was initially assigned to be the value of the 1° cell in which it fell. The evaluation of point values of the function from the degree 360 expansion revealed spurious patterns attributed to the coefficients from degree 181 to 360. Expansion of the original function in 1° cells to degree 180 showed no problems in the point evaluation. Mean 1° values computed from both degree 180 to 360 expansions showed close agreement with the original function. The artifacts could be removed if the 30' values were interpolated by spline procedures from adjacent 1° cells. These results led to an examination of the gravity anomalies and geoid undulations from EGM96 in areas where 1° values were 'split up' to form 30' cells. The area considered was 75°S to 85°S, 100°E to 120°E where the split up cells were basically south of 81°S. A small, latitude related, and possibly spurious effect might be detectable in anomaly variations in the region. These results suggest that point values of a function computed from a high degree expansion may have spurious signals unless the cell size is compatible with the maximum degree of expansion. The spurious signals could be eliminated by using a spline interpolation procedure to obtain the 30' values from the 1° values.

INTRODUCTION

The representation of a function in a spherical harmonic series has been discussed many times in the literature. Expansion of functions such as the Earth's geopotential, topography, dynamic ocean topography, magnetic field, etc., have been carried out to increasingly high degree. In the case of the geopotential, various data types are used to calculate the spherical harmonic representation and quantities such as gravity anomalies, geoid undulations and gravity gradients, can be derived on and above the surface of the Earth. A recent combination solution to degree 360 is described in Lemoine et al. (1998). Tailored geopotential models to degree 1800 have been described by Wenzel (1998).

A case simpler than the representation of a geopotential model is the representation of a function given on the surface of the sphere. For example, representation of the Earth's topography to degree 1800 has been carried out by Balmino (1993). An expansion of the dynamic ocean topography (DOT) to degree 360 has been described by Rapp (1998). This expansion was more difficult than others because the function was not globally defined as DOT is given in the oceans only.

The estimation of spherical harmonic coefficients of a function given on a sphere (()) can be given simply as (Heiskanen and Moritz, 1967):

$$\begin{Bmatrix} a_{nm} \\ b_{nm} \end{Bmatrix} = \frac{1}{4\pi} \iint_{\sigma} f(\theta, \lambda) P_{nm}(\cos \theta) \begin{Bmatrix} \cos m\lambda \\ \sin m\lambda \end{Bmatrix} d\sigma \quad (1)$$

where the coefficients a_{nm} , b_{nm} are fully normalized and P_{nm} are the fully normalized Legendre functions.

The practical evaluation of (1) is complicated by the fact that the function values are usually given as mean values or as point values on a uniform grid. Numerous studies have been carried out in the estimation of the harmonic coefficients from mean values. Rapp (1977) describes the estimation of potential coefficients from mean anomalies with the introduction of the smoothing parameter developed by Pellinen. Colombo (1981) described the estimation of harmonic coefficients from point or mean values using FFT procedures. He suggested the use of a de-smoothing function that could lead to more accurate coefficient estimation taking into account the sampling error caused by the finite size of the sample cell and the smoothing problem caused by the averaging that takes place in the formation of the mean value. Such averaging makes it more difficult to recover high frequency (or degree) information than low frequency (or degree) information from a mean value. In addition Colombo described some tests taking into account noise in the data sample. The analysis by Colombo led to his suggestion for the use of an empirical set of de-smoothing parameters.

Pavlis (1988, p. 75) also discusses the problems of estimating spherical harmonic coefficients from area mean values. He notes that “the area averages of the surface spherical harmonics do not constitute an orthogonal set of base functions on the sphere, even if sampling is regular and the Nyquist frequency is not exceeded.” Sneeuw (1994) discusses spherical harmonic analysis techniques that have been used with discrete data sets. For many data products, the values are given on an equiangular grid. Sneeuw shows that this leads to the non-orthogonality, in the latitude direction, of the discretized Legendre functions. This suggests problems with the recovery of the harmonic coefficients from such data using orthogonality relationships. Sneeuw and Bun (1996) describe FFT techniques that can be used for the analysis of data on an equiangular grid in a way that discrete orthogonality is obtained. Such a procedure requires the introduction of special functions dependent on latitude.

Jekeli (1996) addresses the problem of coefficient recovery considering aliasing effects. He shows that such effects can create biased coefficient estimates when the quadrature process is used with data given on a regular latitude/longitude data grid. He notes that aliasing effects can be reduced if the spherical cap averages, instead of the equiangular cell averages are used.

Bian and Menz (1998) have recently suggested an improved spherical harmonic analysis in which piecewise linearly interpolated function values replace block mean values in the quadrature analysis. They argue that the use of the linear interpolation can reduce the error on the harmonic coefficient estimation. They also suggest that expansion could be carried to degrees higher than that usually implied by the data grid or cell size (see eq. (3) below).

Rapp (1986) describes a number of tests involving the estimation of potential coefficients derived from generated point and mean values of gravity anomalies generated from a given set of potential coefficients. Tests were made to compare input and recovered harmonic coefficients with different coefficient estimation techniques. The tests were carried out to degree 180 only. One of the procedures described in this paper could be represented as follows for a surface function:

$$\begin{Bmatrix} a_{nm} \\ b_{nm} \end{Bmatrix} = \frac{1}{4\pi q_n} \sum_{i=0}^{N-1} \sum_{j=0}^{2N-1} \bar{f}_{ij}(\theta, \lambda) \iint_{\sigma_{ij}} Y_{nm}(\theta, \lambda) d\sigma \quad (2)$$

where

$$\begin{aligned} N &= 180^\circ/\Delta^\circ, \\ \Delta &= \text{angular cell size}, \\ \bar{f}_{ij}(\theta, \lambda) &= \text{mean value of } f(\theta, \lambda) \text{ over cell } (i,j), \\ Y_{nm}(\theta, \lambda) &= \begin{Bmatrix} \cos m\lambda \\ \sin m\lambda \end{Bmatrix} P_n(\cos \theta), \text{ and} \end{aligned} \quad (3)$$

$$q_n = \begin{cases} \beta_n^2 & \text{for } 0 < n \leq \frac{N}{3} \\ \beta_n & \text{for } \frac{N}{3} < n \leq N \\ 1 & \text{for } n > N \end{cases} \quad (4)$$

β_n is a function depending on the cell size and latitude. It is called the Pellinen smoothing operator (eq. (6) in Rapp (1977)).

Additional discussion on this numerical quadrature procedure to recover the harmonic coefficients is given by Pavlis in Section 8.2.1 and 8.5 of Lemoine et al. (1998).

The coefficients estimated from (2) can be used to derive the function value at an arbitrary point or as a mean value over an area σ_{ij} . For the point value we have:

$$f(\theta, \lambda) = \sum_{n=0}^N \sum_{m=0}^n (a_{nm} \cos m\lambda + b_{nm} \sin m\lambda) P_{nm}(\cos \theta). \quad (5)$$

For the mean value we have:

$$\bar{f}_{ij}(\theta, \lambda) = \sum_{n=0}^N \sum_{m=0}^n \frac{a_{nm}}{\sigma_{ij}} \iint_{\sigma_{ij}} \cos m\lambda P_{nm}(\cos \theta) d\sigma + \frac{b_{nm}}{\sigma_{ij}} \iint_{\sigma_{ij}} \sin m\lambda P_{nm}(\cos \theta) d\sigma. \quad (6)$$

For the evaluation of (6) the integral of the Legendre function over specified cell sizes and for selected (e.g. 360) maximum degrees can be computed once and retained. The same values needed in the evaluation of (2) are used in (6).

An interesting calculation is the comparison of computed function values to the original function values used to calculate the harmonic coefficients. The agreement will not be exact because one can not exactly recover the coefficients of data given in finite size cells as noted by Pavlis (1988, Section 4.2.2) and Pavlis (p. 8-6) in Lemoine et al. (1998). As noted by Pavlis (1999, private communication) "the agreement can only be exact if the frequency content of noiseless data does not exceed N-1 and one uses least squares to estimate the coefficients."

An additional point to note is the general limitation that spherical harmonic expansions, should be taken to a degree consistent with the size of the cell in which the function is given. The general relationship is given by (3) where one sees that if the data is given in 1° cells the highest degree of expansion would be about 180. This equation is a guideline only with specific circumstances modifying the validity of the equation.

With the above as preface we can now consider some numerical tests that will show some interesting behavior with implications (perhaps) for the procedures used in the development of the EGM96 degree 360 model.

NUMERICAL RESULTS FOR THE EXPANSION OF A FUNCTION GIVEN IN $1^\circ \times 1^\circ$ CELLS

For this computation we are given a global set of $1^\circ \times 1^\circ$ mean values (64800). The values actually were a component (rad_dot.M2 was the original file name) of post glacial rebound (PGR) rates supplied by Peltier in 1996. The most significant values are in the Hudson Bay region with values becoming smaller away from the region. These sets are displayed and discussed in Peltier (1998, 1999). The type of function used is not pertinent to the results to be described here. The function values were found in the following data set: ZHANGC.SEA.DOT.M2. This file contains ϕ, λ (of the center of the cell) rad_dot.m2 and sea_dot.m2 (the latter value also a component of PGR rates). This file was used to first create a $30' \times 30'$ file where the four $30'$ values within a 1° cell were identical. The values were put in the proper organization for use in a program to be used for the determination of harmonic coefficients from the given values of a function.

The $30'$ values were expanded into a surface spherical harmonic expansion from degree 0 to degree 360 using program RHRAPP.ZHANGC.F419.DOT.MOD1. This program was a modification of the F419 program which was developed by N.K. Pavlis in January 1989. The program primarily uses the HARMIN subroutine developed by Colombo (1981). The program was run with input values considered as $30'$ mean values with the needed integrated associated Legendre functions taken from file 1 of tape CT202. This program uses the de-smoothing parameters defined by (4).

The coefficients were then used in a version of program F388 (RHRAPP.F388.PGR.RATES) to calculate a 0.5 degree grid of values for the Hudson Bay region defined as follows: 55(N to 65(N, 265(to 285(. These values were contoured using program RHRAPP.PLT.PGR.RATES with a contour interval of 1 mm/yr. The resultant plot is Figure 1. The strange patterns of contours was originally pointed out to this author by Hong-Zeng Tseng, a graduate student working with Professor C.K. Shum. This pattern shows the strongest oscillation in the area of the strongest signal. The contour behavior was unexpected since the 30' values in the 1° cell were set to be identical. On the other hand, the values being plotted were point values, not mean values. The pattern of contours indicated an undesirable effect in the recovery of the point function values.

The next step was the construction of a contour plot truncating the 360 expansion to degree 180. Point values were computed on a 0.5 degree grid and contoured as before with the results shown in Figure 2. The pattern here is much smoother than in Figure 1 and much more of what would be expected. It was now clear that the oscillations seen in Figure 1 were attributable to the coefficients from degree 181 to 360.

The original set of 1° x 1° mean values of rad_dot.M2 were now expanded into a spherical harmonic series to degree 180 using RHRAPP.ZHANGC.F419.DOT.FOR180 with the needed integrals of the associated Legendre functions taken from tape GS390 (file 1). These coefficients were then used to create a 0.5 degree function grid which was then contoured and is shown in Figure 3. Comparison of Figures 2 and 3 show little visual difference.

An additional plot was generated using the coefficients of the degree 360 solution from 181 to 360. The results are shown in Figure 4 with a contour interval of 1 mm/yr. This plot would also represent the difference in values shown in Figures 1 and 2. The pattern shown in Figure 4 resembles the pattern seen in Figure 1 indicating that the pattern arises from the coefficients from 181 to 360 as was expected after considering Figures 2 or 3. The largest value plotted in Figure 4 reaches 2.2 mm/yr. The differences fade to zero away from the Hudson Bay test area. This does not mean that the higher frequency effects are negligible outside this area. The clear latitude structures of the pattern seen in both Figures 1 and 4 may be related to the discrete non-orthogonality issue noted in Sneeuw (1994).

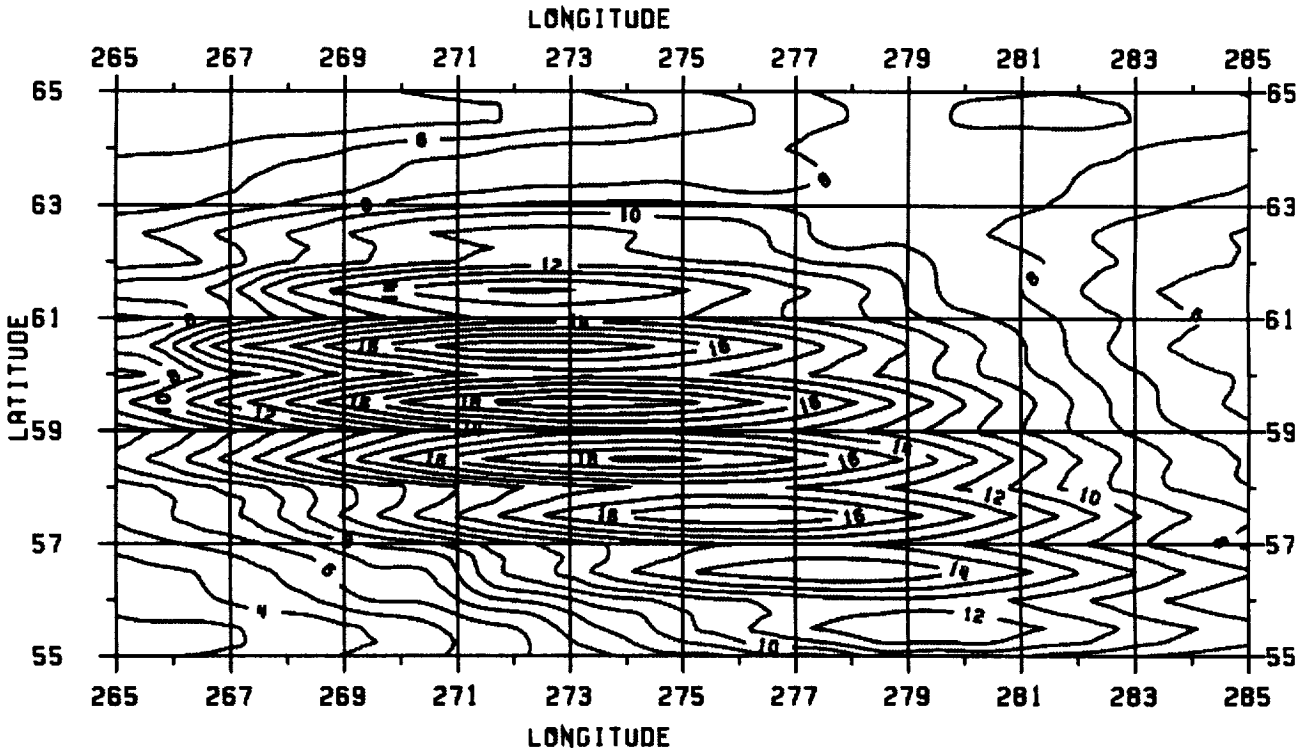


Figure 1. Values of rad_dot.M2 based on a 0.5° grid of point values from the full degree 360 expansion of the 30' mean values. Contour interval is 1 mm/yr.

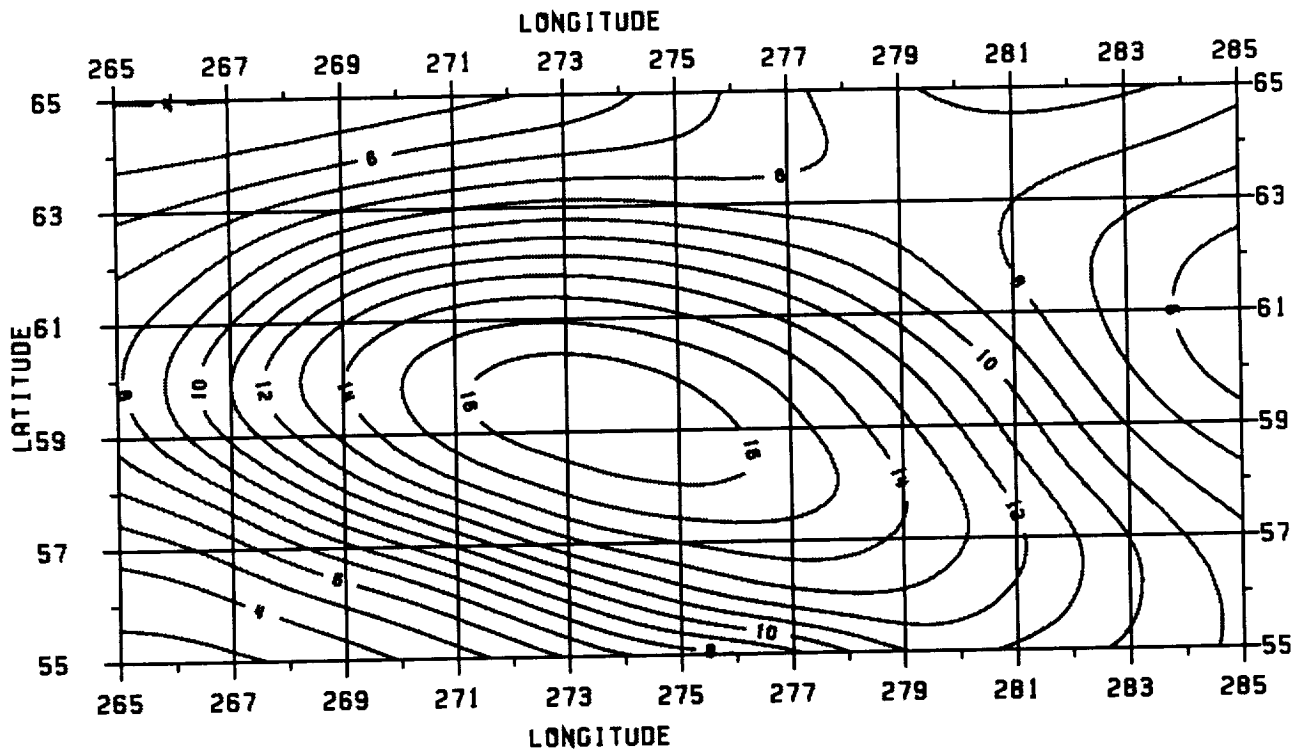


Figure 2. Values of rad_dot.M2 based on a 0.5° grid of point values from the truncated (to 180) degree 360 expansion of the $30'$ mean values. Contour interval is 1 mm/yr.

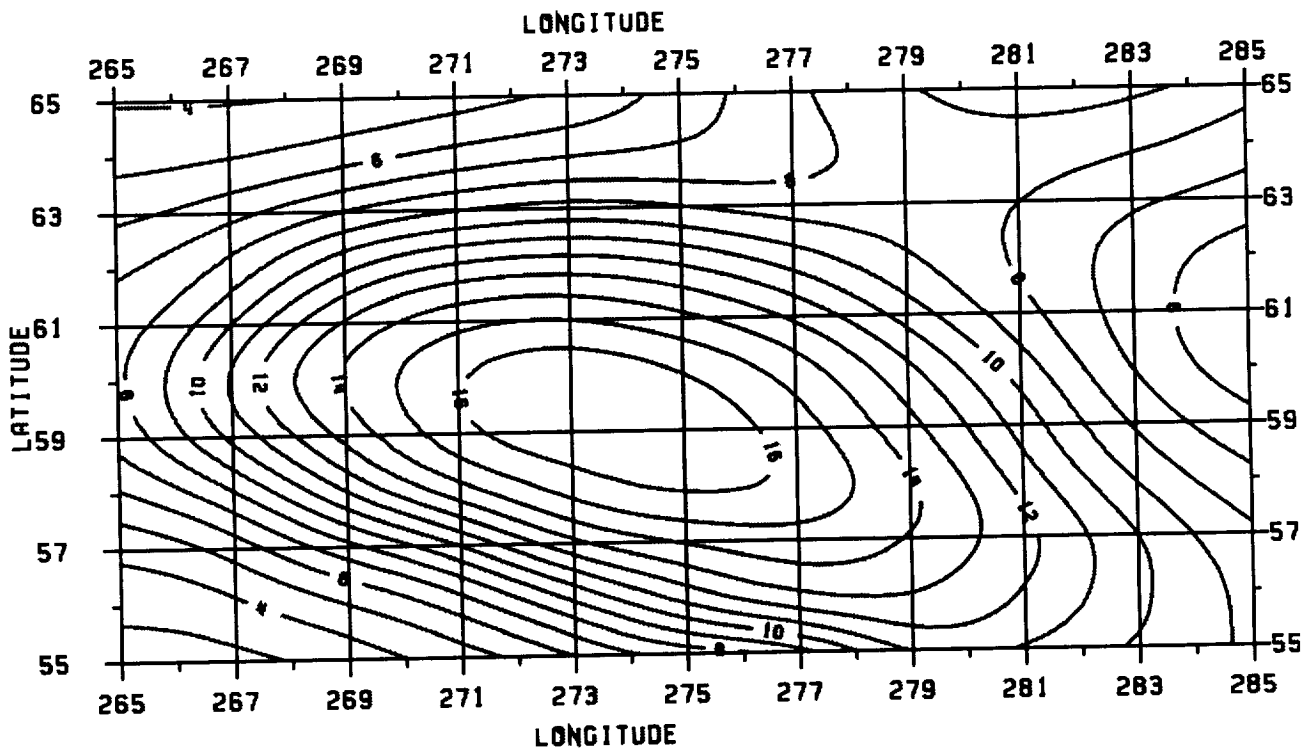


Figure 3. Values of rad_dot.M2 based on a 0.5° grid of point values computed from the degree 180 expansion of the $1^\circ \times 1^\circ$ mean values. Contour interval is 1 mm/yr.

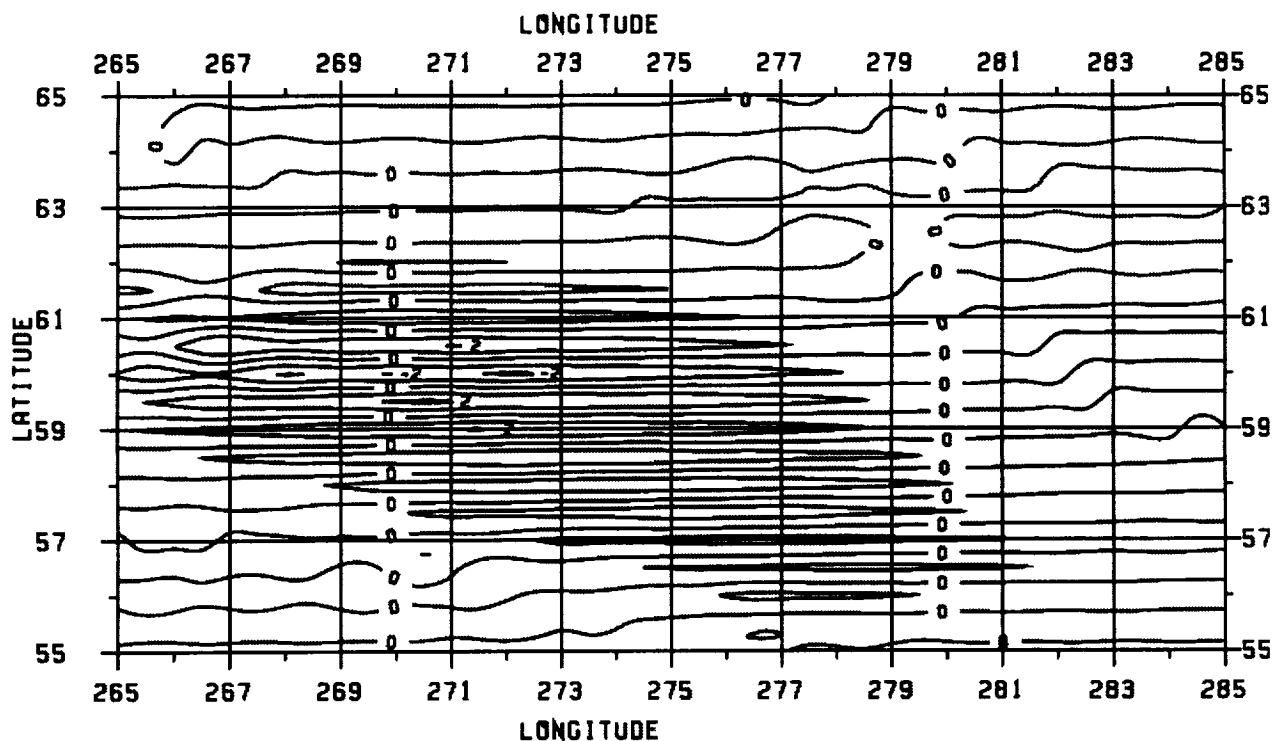


Figure 4. Values of rad_dot.M2 based on a 0.5° grid of point values from degree 181 to 360 expansion of the 30' mean values. Contour interval is 1 mm/yr.

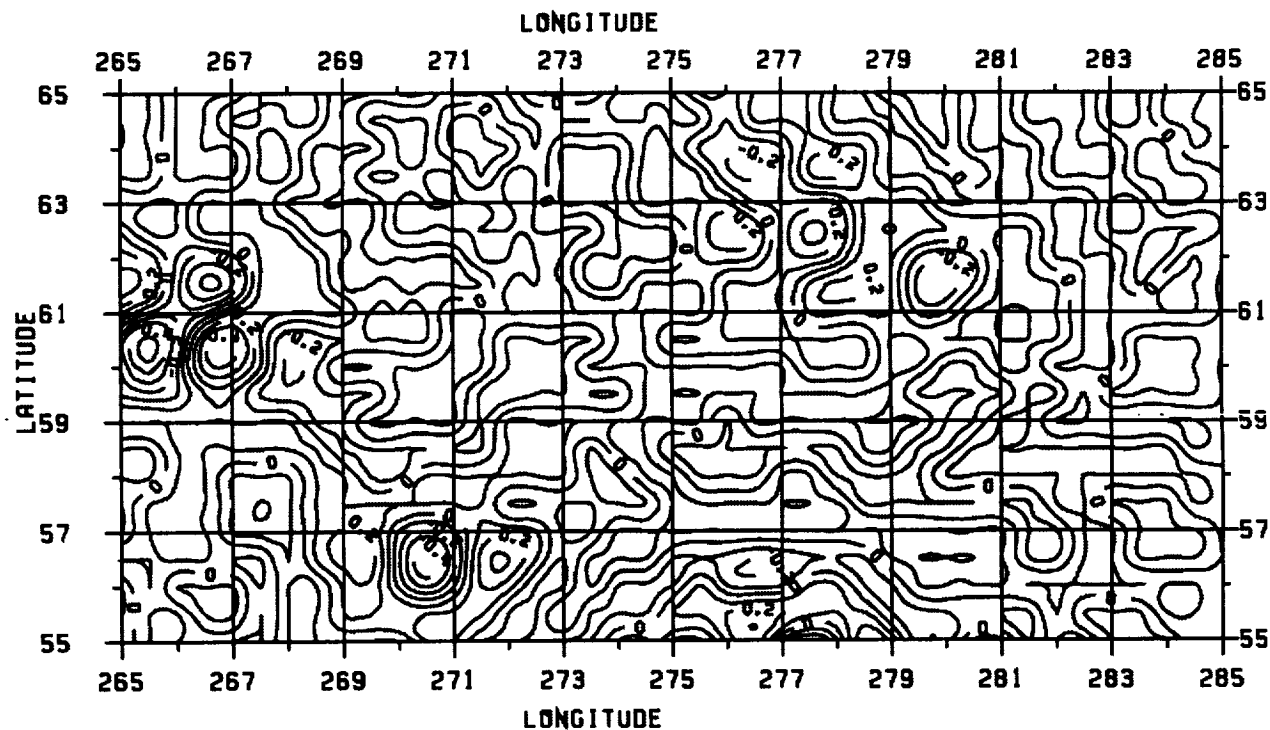


Figure 5. Values of rad_dot.M2 based on a 0.5° grid of point values from the degree 181 to 360 expansion of the 30' spline interpolated mean values. Contour interval is 0.1 mm/yr.

The degree 360 expansion of the spline interpolated values was made using the identical procedures used when the split up 30' values were processed. The function values were then evaluated. A plot similar to Figure 1 was obtained indicating the spurious signals or artifacts seen in Figure 1 were no longer there. Figure 5 shows the value of the function based on the expansion of the 30' spline interpolated values from degree 181 to 360. This figure is analogous to Figure 4 except the contour interval is 0.1 mm/yr not the 1 mm/yr used for Figure 4. This was the first indication that the spline interpolation procedure had basically eliminated the artifact pattern seen in Figures 1 and 4.

From Figure 6 one notes that the center latitude values (57.5° , 60.5°) from the 360 expansion of the $30'$ split up values have a significantly higher magnitude than the values at the upper or lower latitude limits of the cell. Such variations are not seen in the longitude direction. This behavior creates

Figure 6. Point values of rad_dot.M2 from degree 360 (30' direct) (top value), degree 180 (1° data) (middle value) and degree 360 (30' spline) (lower value) expansion on a 30' grid. Units are mm/yr.

The next issue was how well did the expansions represent the input data. In this case we considered the 1° data to be the basic value. The mean value in a cell was computed using eq. (6) with program RHRAPP.F431.NKP.PGR.ONE DEG. Although the computation was done globally, comparisons were made for just four 1° cells in the study region. The results are given in Table 1.

Table 1.
1° x 1° Mean Values of rad_dot.M2 Computed From Five Spherical Harmonic
Expansions. Units are mm/yr

Value	Latitude and Longitude of 1° Cell's Northwest Corner			
	61°N 270°E	58°N 270°E	58°N 276°E	59°N 273°E
Original Value	14.36	10.99	14.70	15.58
1° to 180	14.38	10.95	14.70	15.62
30' to 360/to 180 only	14.25	10.91	14.58	15.47
30' to 360 complete*	14.32	10.96	14.67	15.54
30' to 360/to 180 only†	14.30	10.92	14.63	15.53
30' to 360 complete†	14.31	10.93	14.66	15.54

* direct 30' split up † 30' spline

From these numbers one sees that the original value is not duplicated by any solution as was expected. For three of the four cells the value computed from the 1° expansion to degree 180 agrees best with the original mean value although differences are small with the other expansions. The 1° mean value from both degree 360 solutions are virtually the same. The degree 180 part of the 360 expansion of the split up 30' values gives values that are smaller than the 360 values reflecting the signal content from 181 to 360. On the other hand the 180 part of the 360 expansion of the 30' spline value is very close to the full 360 expansion reflecting little contribution from 181 to 360.

This discussion is based on only four cells. More comprehensive studies could be done for all 64800 values to form a comprehensive analysis. This was not done here as the function being studied had maximum values in a specific geographic region (Hudson Bay) with values away from this area being much smaller. If such analysis is considered important it might be done with a global elevation/depth file.

We next considered the power in each of the expansions. We computed the degree variances from the usual equation:

$$\sigma_n^2 = \sum_{m=0}^n (a_{nm}^2 + b_{nm}^2). \quad (7)$$

The square root of the power for various solutions is given in Table 2.

Table 2.
Square Root of Spectral Power and Differences for Various Expansions of rad_dot.M2.
Units are mm/yr

Solution	Value
1°x1° Weighted RMS Value (original data)	1.211
Degree 0 to 360, 30' direct split up	1.218
Degree 0 to 360, 30' spline interpolation	1.218
Degree 0 to 180, 30' direct split up	1.216
Degree 0 to 180, 30' spline interpolation	1.218
Degree 0 to 180 of 1°x1° expansion	1.222
Degree 181 to 360, 30' direct split up	0.063
Degree 181 to 360, 30' spline interpolation	0.006
Degree 0 to 180, 30' direct vs. 30' spline	0.004
Degree 181 to 360, 30' direct vs. 30' spline	0.005
Degree 0 to 180, 1° x 1° vs. 30' direct	0.011
Degree 0 to 180, 1° x 1° vs. 30' spline	0.008

From Table 2 we first see that the root mean square total magnitude from all the expansions is close to the actual root mean square value of the $1^\circ \times 1^\circ$ value computed using cosine weighting. However, the power from degree 181 to 360 is far more (0.063 vs. 0.006 mm/yr) in the case of the direct split up $30'$ values as opposed to the spline interpolated values. A comparison of the degree 180 expansion of the $1^\circ \times 1^\circ$ values to the 180 part of the degree 360 expansion of the split up values and of the $30'$ spline interpolated values shows a smaller difference with the latter solution (0.011 vs. 0.008 mm/yr).

The additional power (0.063 mm/yr) in the 360 expansion of the direct split up values from 181 to 360 seems small but we do know that this contribution can have significant effects in localized regions (see Figure 4). The effects in the Hudson Bay region reach 2 mm/yr (Figure 4), 32 times the root mean square global value.

This analysis indicates that the expansion of a function given initially as 1° values into a degree 360 expansion, by using four $30'$ values identical to a 1° value, can lead to unrealistic variations of the point functions computed from the degree 360 expansion. The problem primarily occurs in the coefficients from degree 181 to 360. On the other hand, if the $30'$ values are interpolated with a spline procedure the resultant degree 360 expansion gives a smooth function representation with none of the artifacts seen when the split up $30'$ values are used. One finds that the power from degree 181 to 360 is 90% less in the case of the $30'$ spline interpolated values versus the $30'$ values from the split up procedure. The increased power should be related to the use of a step function representation of the function value instead of the much smoother and more continuous spline interpolated values.

Clearly the results described here are based on limited numerical tests. Additional insight could be found by expanding some global function that could be defined as both 1° and $30'$ values. A good example would be the JGP95E elevation file.

EXAMINATION OF THE EGM96 GEOPOTENTIAL MODEL FOR SOLUTION ARTIFACTS IN POINT VALUES

In the estimation of the EGM96 geopotential model, as well as some earlier Ohio State models (OSU89A/B, OSU91A), $30'$ mean gravity anomalies were a primary data type. In some cases $30'$ values were not available but 1° values were. In this case the 1° value was "split-up" into four $30'$ values with each $30'$ value given the same value as the 1° , as described by Pavlis in Section 8.3 (p. 8-16) of Lemoine et al. (1998). The total number of $30'$ values, based on 1° values, was 6500. The split up anomalies used in EGM96 cover only 0.74% of the Earth's surface in contrast to the OSU91A model in which 7.95% of the surface was represented by split up anomalies (Rapp et al., 1991, Table 19). Figure 8.3-1 (page 8-21) in Lemoine et al. (1998) graphically identified the types of $30'$ mean anomalies used in the merged file. From this plot we visually estimated that $30'$ from 1° anomalies were used in the region 81°S to 85°S , 105°E to 120°E . (A plot showing the location of the split up anomalies used in the EGM96 development is given in the Appendix). For the first set of computations these limits were expanded to 75°S to 85°S , 100°E to 120°E to be consistent with the angular size of the region used in the rad_dot tests. The split up values occur primarily below 80°S except for a strip of directly estimated $30'$ values at center longitude 106.75°E .

Figure 7 shows the gravity anomalies and Figure 8 shows the geoid undulations based on the EGM96 potential coefficients from degree 181 to 360 in the test area. These values have been computed on a 0.5° grid using program RHRAPP.F388.EGM96.ASCII. The anomaly contour interval is 4 mGals and the undulation contour interval is 10 cm. The anomaly plot (Figure 7) shows significant high frequency signal in the region 78°S , 106°E (roughly). The anomalies in this region came from "observed" $30'$ values. The high frequency effects are substantial. Near 78.5°S , 102°E the residual is 32 mGals changing to -28 mGals near 79.5°S , 103°E . From 78°S , 105.2°E (residual equals -36 mGals) to 77.5°S , 109°E (residual equals 41 mGals) we see a total change of 77 mGals which is large. Similar large changes are seen in the undulation plot (Figure 8). At 78.5°S , 102°E the residual is 100 cm changing to -80 cm at 79.5°S , 103°E . The undulation change clearly reflects the local anomaly behavior. The consideration of these high frequency effects is beyond the scope of this report where we are primarily interested in the effect in and around the cells in which the $30'$ values were assigned based on the 1° split up. The pattern seen in Figure 4 is not as apparent in Figures 7 and 8. To examine this further computations were made for the region 81°S to 83°S , 107°E to 109°E .

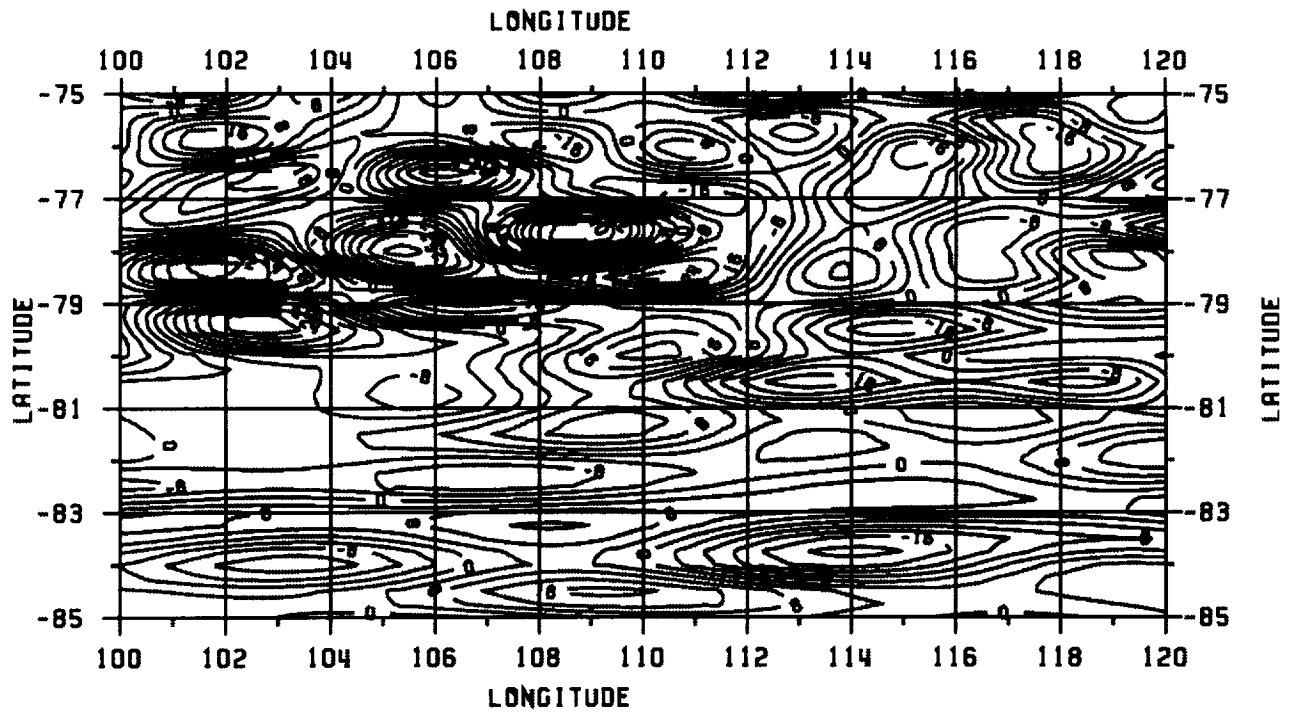


Figure 7. Values of gravity anomaly contribution from degree 181 to 360 from EGM96.
Contour interval is 4 mGal.

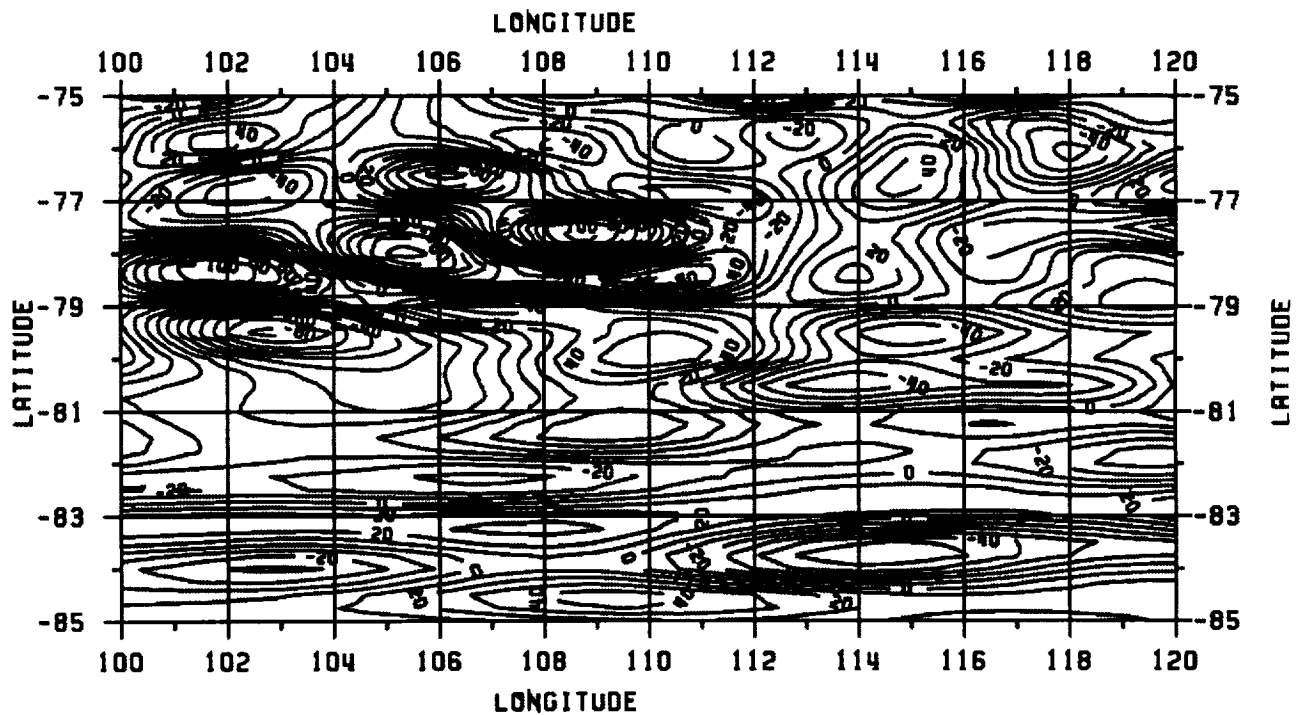


Figure 8. Values of geoid undulation contribution from degree 181 to 360 from EGM96.
Contour interval is 10 cm.

For this $2^\circ \times 2^\circ$ region, that contained 1° to $30'$ split up anomalies, the anomaly values were computed on a 0.25° grid from EGM96. These anomalies are shown in Figure 9 with a 2 mGal contour interval. One sees a significant point value variation over each 1° cell. This variation represents, in part, the interpolation procedure inherent in the spherical harmonic expansion. There is a hint at a latitude dependent effect with the contour pattern near 81.5°S and 82.5°S . The anomaly contribution from degrees 181 to 360 is shown in Figure 10 and the geoid undulation contribution (181 to 360) is shown in Figure 11. Significant variation of these high frequency effects across the 1° cell are seen. Part of this variation is the spherical harmonic interpolation process. But there is a hint of a latitude effect that is similar to that seen in Figure 4.

One should note that in plots such as Figures 7, 8, 10, and 11 there is an assumption made that effects associated with wavelengths below that implied by the use of 1° data are represented by the harmonics from degree 181 to 360. This assumption is consistent with Equation (3) or the $180^\circ/\Delta^\circ$ rule. However, this equation is an approximation only and so therefore is our use of the coefficients from 181 to 360 as representation of high frequency effect associated with $30'$ mean values.

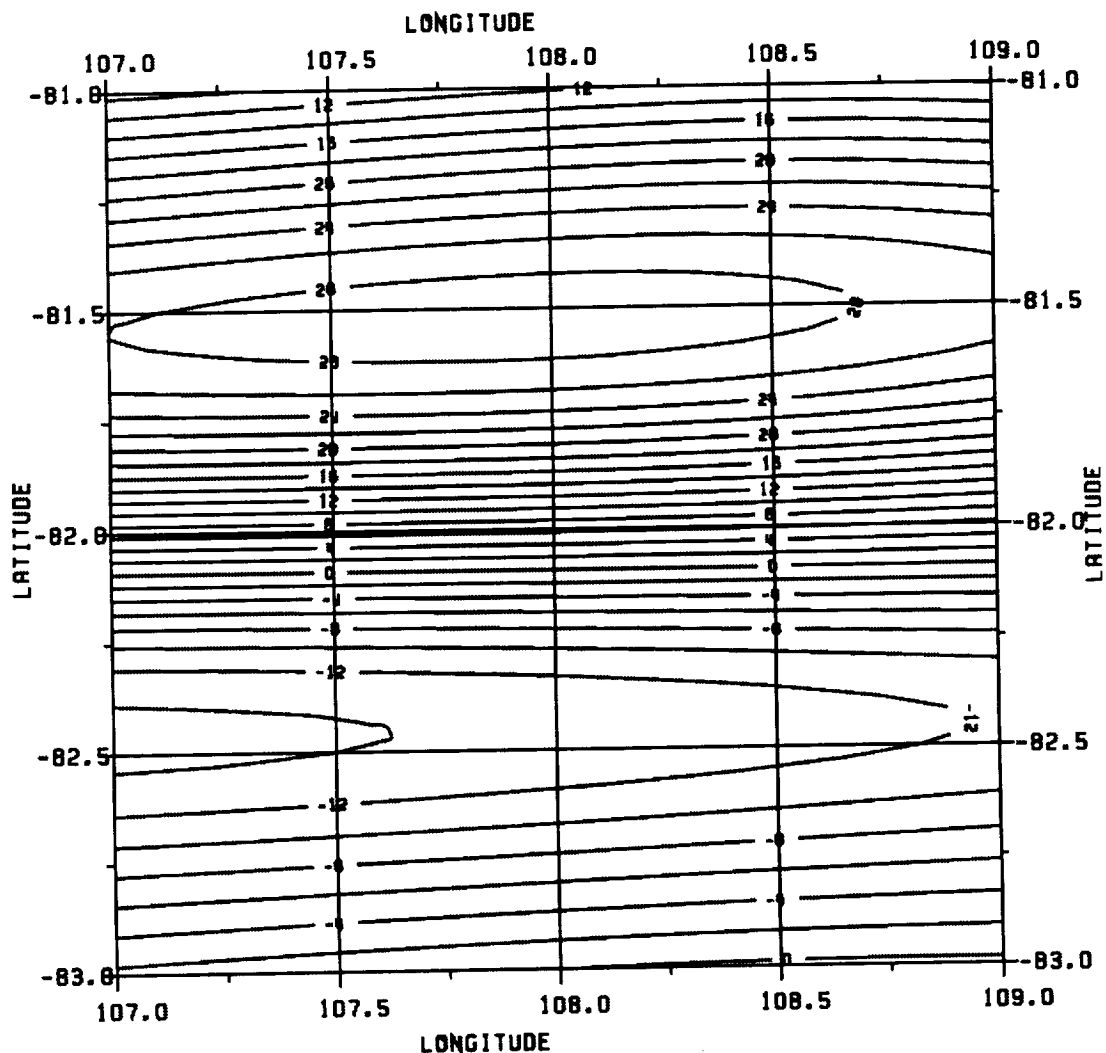


Figure 9. Value of the gravity anomaly from the EGM96 geopotential model in a small Antarctic region. Contour interval is 2 mGal.

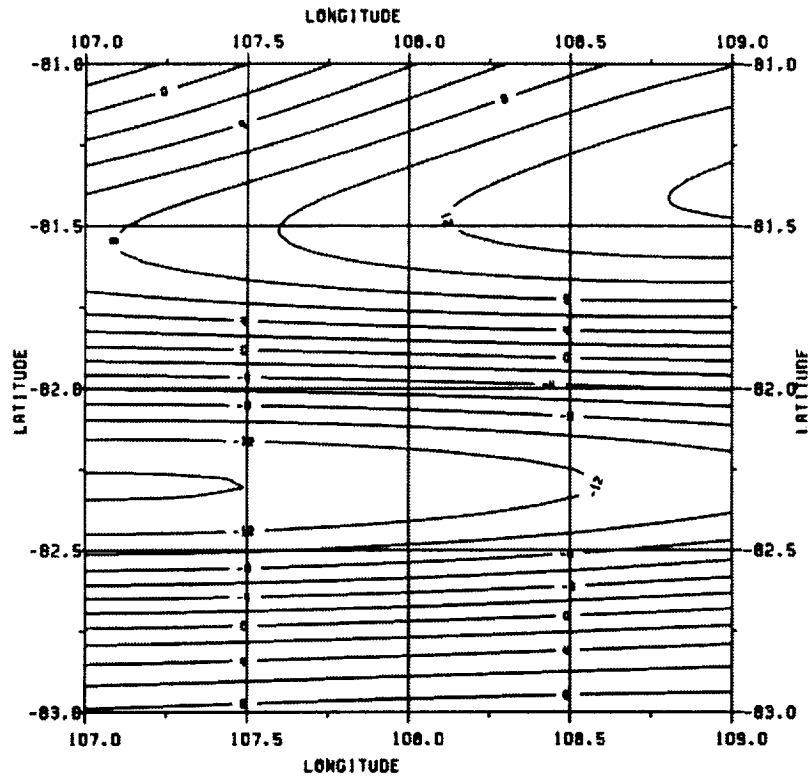


Figure 10. Value of the gravity anomaly contribution from degree 181 to 360 from EGM96 in a small Antarctic region. Contour interval is 2 mGal.

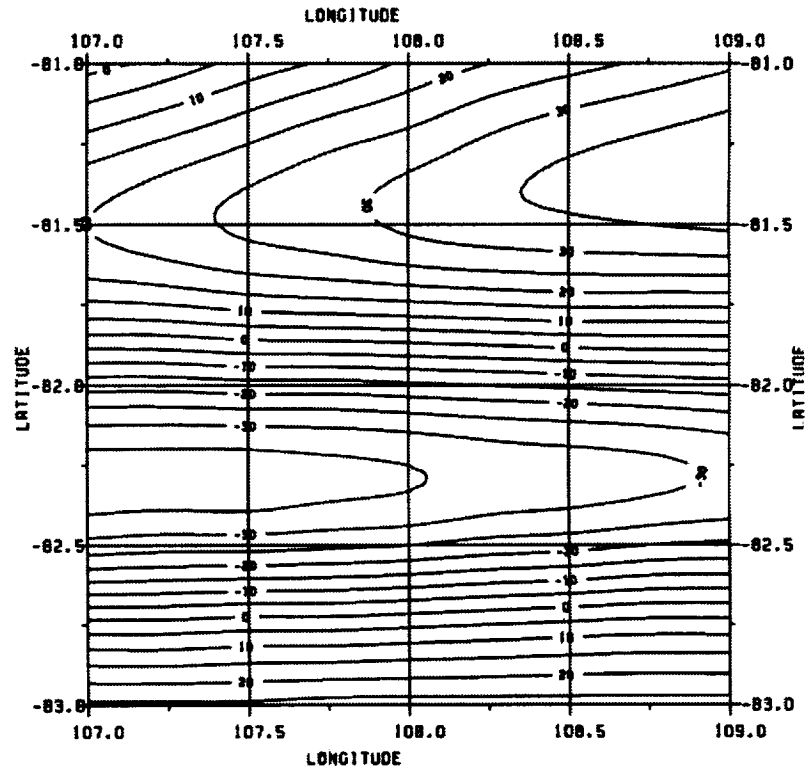


Figure 11. Value of the geoid undulation contribution from degree 181 to 360 from EGM96 in a small Antarctic region. Contour interval is 5 cm.

In order to put these results with EGM96 into context plots have been constructed in a region (40°N to 42°N, 254°E to 256°E) of the United States in which the anomalies used in EGM96 are 30' directly estimated values and for which there is a substantial anomaly variation. By directly estimated we mean a value calculated from point gravity values as described by Kenyon (Section 3.3.3) in Lemoine et al. (1998). The approximate free-air anomaly values in this area have been provided by Pavlis (1999, private communication) and are given in Table 3. They are approximate as these are values before the downward continuation correction (Pavlis (Section 8.3) in Lemoine et al. (1998)) was applied. Such a correction is less than one mGal. In addition, the anomaly calculated from EGM96 is not directly comparable to the value given in Table 3, since EGM96 reflects the combination of satellite and terrestrial data while the data in Table 3 is the terrestrial component that went into the adjustment. However, since the anomalies in this area have a high accuracy, the values from Table 3 and those computed from EGM96 should be comparable to the extent now discussed.

Figure 12 shows the free-air gravity anomaly (more precisely, the radial component) computed from the EGM96 geopotential model. The point values have been computed on a 0.25° grid and contoured with a 10 mGal contour interval. Grid lines have been drawn to show 30' cells. Clearly seen is the significant variation in the 30' cell. For example, for the cell whose center is at 40.75°N, 254.75°E, one sees anomaly variations from -26 mGal to 80 mGal. The given input value was 25 mGal which is close to the mean value of the anomalies shown in Figure 12. Similar effects are seen for the other cells. Although the information given to the solution process for EGM96 gives just a 30' mean value we see significant variation of point value of the function across the cell. However the mean value of the point function will approximate the given input value. The function contoured in Figure 12 displays none of the artifacts seen in Figure 1 where a 360 expansion of split up 1° to 30' values was used. One sees an apparently well behaved interpolation process that is implied by the degree 360 expansion that uses directly estimated 30' values as input data.

Table 3.
30' Free-Air Anomalies in US Test Area

Position of 30' Cell Center		Free-Air Anomaly
Latitude (°N)	Longitude (°E)	(mGal)
41.75	254.25	58
41.75	254.75	66
41.75	255.25	6
41.75	255.75	-15
41.25	254.25	65
41.25	254.75	61
41.25	255.25	-3
41.25	255.75	-4
40.75	254.25	96
40.75	254.75	25
40.75	255.25	-15
40.75	255.75	-7
40.25	254.25	91
40.25	254.75	-3
40.25	255.25	-38
40.25	255.75	-19

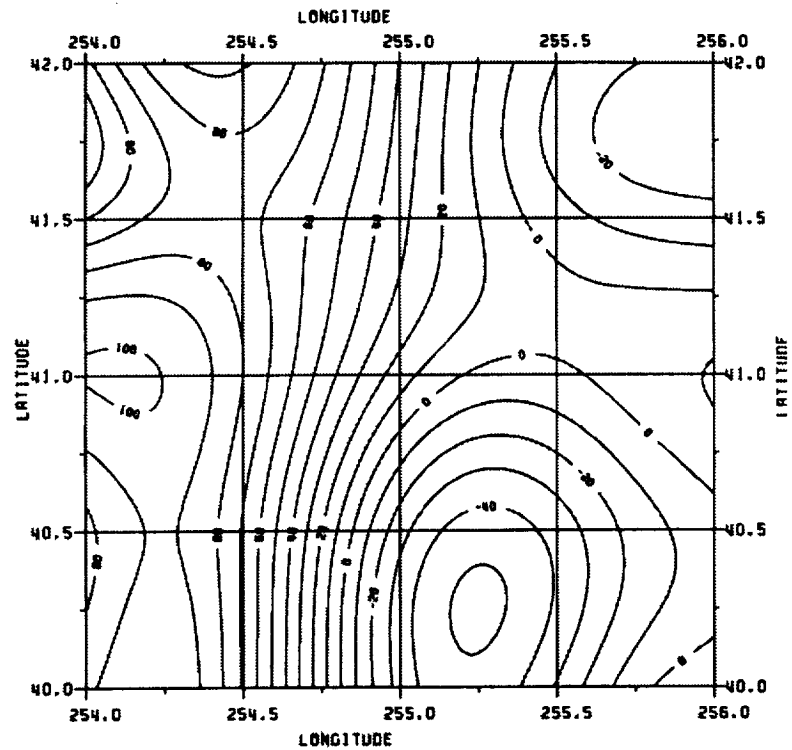


Figure 12. Value of the gravity anomaly from EGM96 in a US test region
Contour interval is 10 mGal.

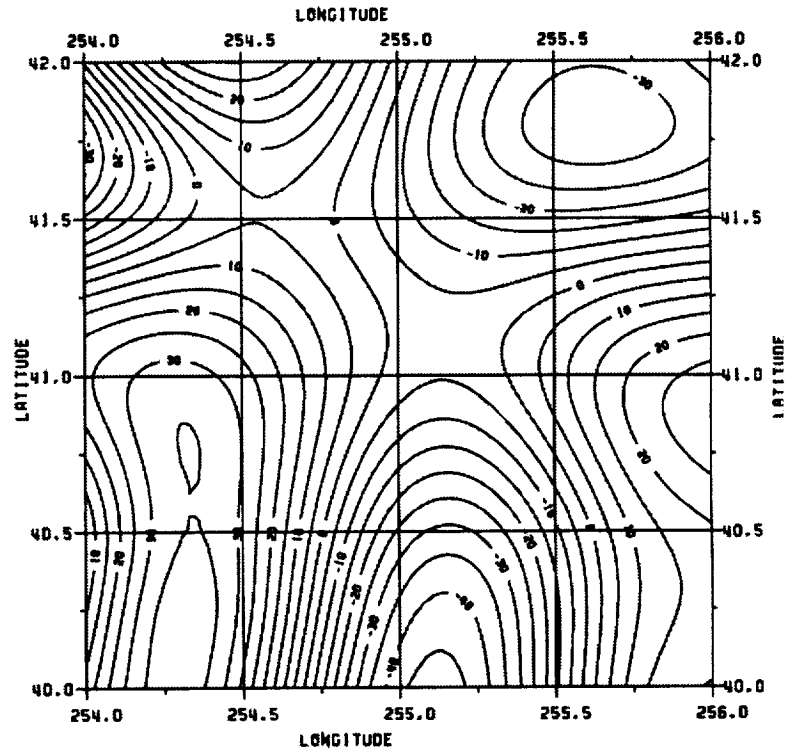


Figure 13. Value of the gravity anomaly contribution from degree 181 to 360 from EGM96 in a US test region.
Contour interval is 5 mGal.

Figure 13 shows the anomaly information, on a 0.25° grid, in the same region based on degrees 181 to 360 of EGM96. The magnitude of the anomaly is significantly less, in some cases, than seen in Figure 12. However, one still sees the variations across the $30'$ cells. These variations do not display, however, the latitude dependent artifacts seen in Figure 1 (for rad_dot values) nor in Figure 11 for anomalies in an area in the Antarctic where 1° to $30'$ split up anomalies were used.

Finally, one should note that the estimation of EGM96 above degree 70 was based primarily on a block diagonal least squares estimation process as described by Pavlis (Section 8.2.2) in Lemoine et al. (1998). The coefficients at degree 360 did originate from a quadrature expansion. Tests are needed to see if the block diagonal procedure, with split up anomalies, generates the artifacts seen when the quadrature procedure is used.

CONCLUSIONS

This study considered the expansion of functions into spherical harmonic series to a degree higher than implied by the cell size in which the function was originally given. In the first case studied 1° cells were broken into $30'$ cells that were expanded into a degree 360 set of harmonic coefficients. When the expansion was used to evaluate point values of the function artificial variations across the 1° cell were generated. Evaluation of the function using coefficients from degree 181 to 360 showed the irregular variations were associated with the higher degree effects. When the original function, given in 1° cells was expanded into a degree 180 series, the point function, evaluated from these coefficients showed that no artificial signals. Mean 1° values were calculated from various expansions with all values agreeing closely with the original input data.

Instead of doing a direct split up of the 1° values to $30'$ values, another procedure was tested in which the $30'$ values were interpolated from the 1° values using a spline interpolation process. When these values were expanded into a spherical harmonic series with the resultant function evaluated, no artifact signal was seen. It was found that the square root of the power contained in the expansion of the spline interpolated $30'$ values, in the degree range 181 to 360, was only 10% of that found when using the direct 1° split up. This implied that the spline interpolation procedure created a field sufficiently smooth to in essence filter out the unwanted and spurious high (181 to 360) frequency effects.

A second study considered the EGM96 model. A study area was determined that had $30'$ anomalies created by the split up of 1° surface gravity values. Values of gravity anomalies and geoid undulations were computed both from the full field and from degree 181 to 360. Patterns of behavior for the point functions seen in the first study were hinted at in the regions where the split up values were used. Significant anomaly and undulation variations were seen across the 1° cell in which the four $30'$ input values to the EGM96 solution were all equal.

Computation were also made for a $2^\circ \times 2^\circ$ test region in the U.S. where no split up anomalies were used in the EGM96 solution. The anomalies showed significant variation across the $30'$ cells although the mean value would closely match the input data. (Exact agreement would not be expected because of the adjustment process carried out with satellite derived normal equations). The variations did not appear to show the artifacts noted with the first analyses of rad_dot values (1° to $30'$) nor the apparent latitude effects seen in EGM96 in a split up (1° to $30'$) region.

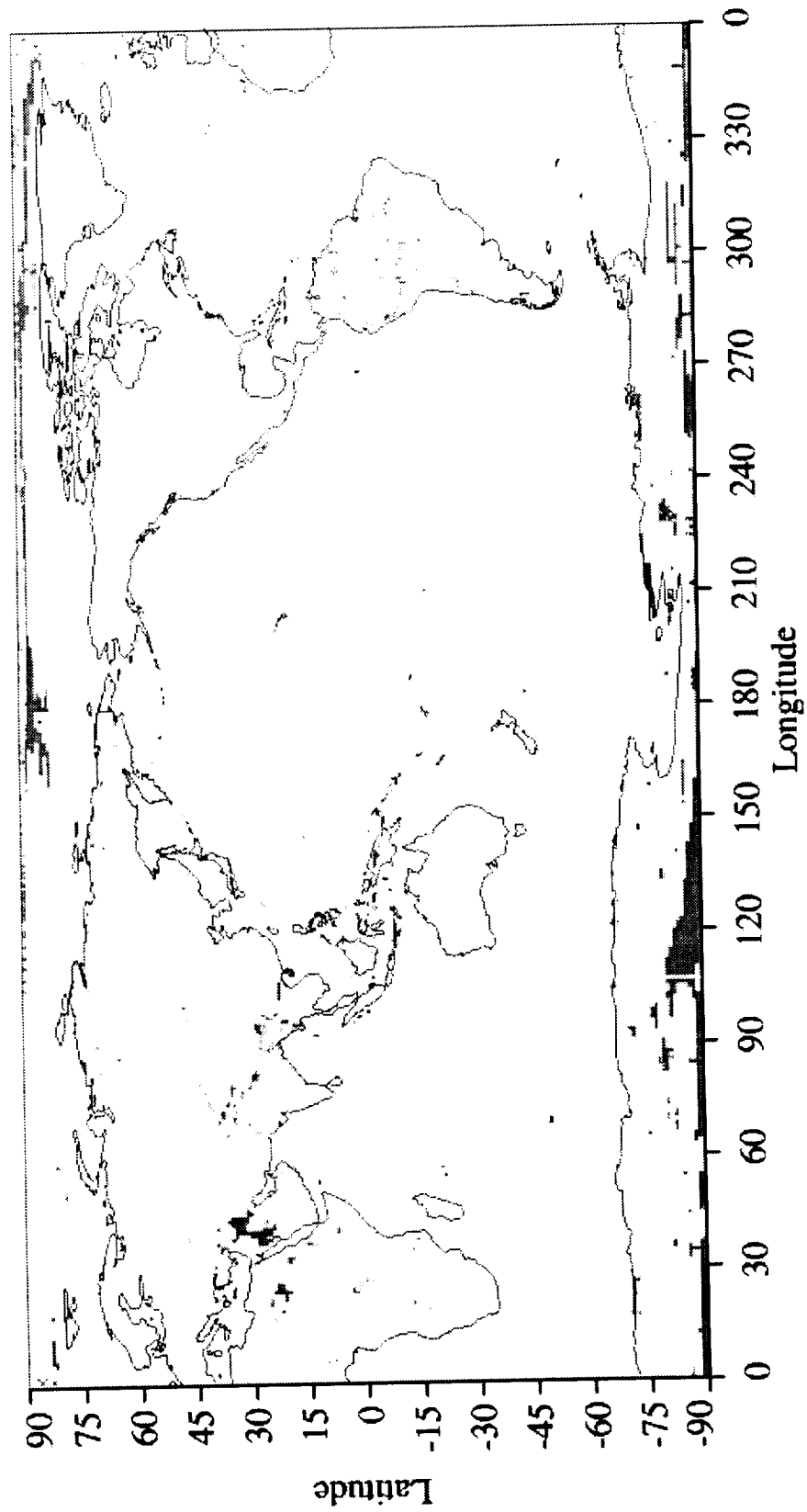
The results presented in this report suggest that point values computed from a degree 360 expansion must be used with caution in regions where anomaly split up values were used. The point variations may not be real and are probably simple artifacts of the solution technique. A simple technique to eliminate the problem would be to interpolate the $30'$ values from surrounding 1° or $30'$ values using a spline interpolation procedure. Additional tests using the block diagonal estimation procedure, as used for the estimation of EGM96, would be helpful.

The results suggest that improved ways for estimating high degree solutions are sought when the data cell size is not consistent with the highest degree of the expansion sought. In fact improved procedures, considering the results of recent papers noted in the text, should be developed.

REFERENCES

- Balmino, G., The spectra of the topography of the Earth, Venus and Mars, *Geophy. Res. Letters*, 20(11), 1063-1066, 1993.
- Bian, S., and J. Menz, Using piecewise linear interpolations in spherical harmonic analyses, *J. Geodesy*, 72: 473 - 481, 1998.
- Columbo, O.L., Numerical methods for harmonic analysis on the sphere, *Rep. 310*, Dept. of Geod. Sci. and Surv., Ohio State Univ., Columbus, 1981.
- Heiskanen, W.A. , and H. Moritz, *Physical Geodesy*, W.H. Freeman and Co., San Francisco, 1967.
- Jekeli, C., Spherical harmonic analysis, aliasing, and filtering, *J. Geodesy*, 70:214-223, 1996.
- Lemoine, F.G., S.C. Kenyon, J.K. Factor, R.G. Trimmer, N.K. Pavlis, D.S. Chinn, C.M. Cox, S.M. Klosko, S.B. Luthcke, M.H. Torrence, Y.M. Wang, R.G. Williamson, E.C. Pavlis, R.H. Rapp, and T.R. Olson, The Development of the Joint NASA GSFC and the National Imagery and Mapping Agency (NIMA) Geopotential Model EGM96, NASA/TP-1998-206861, Goddard Space Flight Center, Greenbelt, MD, 1998.
- Pavlis, N.K., Modeling and estimation of a low degree geopotential model from terrestrial gravity data, *Rep. 386*, Dept. of Geod. Sci. and Surv., Ohio State Univ., Columbus, 1988.
- Peltier, W. R., Postglacial variations in the level of the sea: Implications for climate dynamics and solid earth geophysics, *Reviews of Geophysics*, 36(4), 603-689, 1998.
- Peltier, W. R., Global sea level rise and glacial isostatic adjustment, *Global and Planetary Change*, in press, 1999.
- Rapp, R.H., The relationship between mean anomaly block sizes and spherical harmonic representation, *J. Geophys. Res.*, 82 (33), 5360-5364, 1977.
- Rapp, R.H., Global geopotential solutions, in *Lecture Notes in Earth Science*, Vol. 7, Mathematical and Numerical Techniques in Physical Geodesy, ed. by Suenkel, Springer-Verlag, 365 - 114, 1986.
- Rapp, R.H., The development of a degree 360 expansion of the dynamic ocean topography of the POCM_4B global circulation model, NASA/CR-1998-206877, Goddard Space Flight Center, Greenbelt, MD, 1998.
- Rapp, R.H., Y.M. Wang and N.K. Pavlis, The Ohio State 1991 geopotential and sea surface topography harmonic coefficient models, *Rep. 410*, Dept. of Geod. Sci. and Surv., Ohio State Univ., Columbus, 1991.
- Sneeuw, N., Global spherical harmonic analysis by least-squares and numerical quadrature methods in historical perspective, *Geophy. J. Int.*, 118, 707 - 716, 1994.
- Sneeuw, N., and R. Bun, Global spherical harmonic computation by two-dimensional Fourier methods, *J. Geodesy*, 70: 224 - 232, 1996.
- Wenzel, H.G., Ultra high degree geopotential model GPM3E97A to degree and order 1800 tailored to Europe, in *Proc. of Second Continental Workshop on the Geoid in Europe*, Reports of the Finish Geodetic Institute, 98:4 (Vermeer and Adam (eds.)), 1998.

APPENDIX



Geographic location of the 6500 30'x30' cells (gray areas) where the gravity anomaly values used in the development of EGM96 originated from the split up of 1°x1° data (Pavlis, private communication, 1999)

REPORT DOCUMENTATION PAGE			Form Approved OMB No. 0704-0188	
Public reporting burden for this collection of information is estimated to average 1 hour per response, including the time for reviewing instructions, searching existing data sources, gathering and maintaining the data needed, and completing and reviewing the collection of information. Send comments regarding this burden estimate or any other aspect of this collection of information, including suggestions for reducing this burden, to Washington Headquarters Services, Directorate for Information Operations and Reports, 1215 Jefferson Davis Highway, Suite 1204, Arlington, VA 22202-4302, and to the Office of Management and Budget, Paperwork Reduction Project (0704-0188), Washington, DC 20503.				
1. AGENCY USE ONLY (Leave blank)		2. REPORT DATE June 1999		3. REPORT TYPE AND DATES COVERED Contractor Report
4. TITLE AND SUBTITLE Artifacts Introduced in the Point Evaluation of Functions Expanded into a Degree 360 Spherical Harmonic Series			5. FUNDING NUMBERS NAS5-32352	
6. AUTHOR(S) R. Rapp				
7. PERFORMING ORGANIZATION NAME(S) AND ADDRESS (ES) Goddard Space Flight Center Greenbelt, Maryland 20771			8. PERFORMING ORGANIZATION REPORT NUMBER 99B00046	
9. SPONSORING / MONITORING AGENCY NAME(S) AND ADDRESS (ES) National Aeronautics and Space Administration Washington, DC 20546-0001			10. SPONSORING / MONITORING AGENCY REPORT NUMBER CR—1999—209229	
11. SUPPLEMENTARY NOTES				
12a. DISTRIBUTION / AVAILABILITY STATEMENT Unclassified - Unlimited Subject Category: 64 Report available from the NASA Center for AeroSpace Information, Parkway Center/7121 Standard Drive, Hanover, Maryland 21076-1320			12b. DISTRIBUTION CODE	
13. ABSTRACT (Maximum 200 words) An expansion of a function initially given in 1° cells was carried out to degree 360 by using 30' cells whose value was initially assigned to be the value of the 1° cell in which it fell. The evaluation of point values of the function from the degree 360 expansion revealed spurious patterns attributed to the coefficients from degree 181 to 360. Expansion of the original function in 1° cells to degree 180 showed no problems in the point evaluation. Mean 1° values computed from both degree 180 to 360 expansions showed close agreement with the original function. The artifacts could be removed if the 30' values were interpolated by spline procedures from adjacent 1° cells. These results led to an examination of the gravity anomalies and geoid undulations from EGM96 in areas where 1° values were "split up" to form 30' cells. The area considered was 75 °S to 85°S, 100° E to 120° E where the split up cells were basically south of 81 °S. A small, latitude related, and possibly spurious effect might be detectable in anomaly variations in the region. These results suggest that point values of a function computed from a high degree expansion may have spurious signals unless the cell size is compatible with the maximum degree of expansion. The spurious signals could be eliminated by using a spline interpolation procedure to obtain the 30' values from the 1° values.				
14. SUBJECT TERMS Numerical Analysis, Geophysics, Oceanography			15. NUMBER OF PAGES 19	
			16. PRICE CODE	
17. SECURITY CLASSIFICATION OF REPORT Unclassified	18. SECURITY CLASSIFICATION OF THIS PAGE Unclassified	19. SECURITY CLASSIFICATION OF ABSTRACT Unclassified	20. LIMITATION OF ABSTRACT UL	

